2025
12(2), 1261

Chemical Biology
LETTERS

Discovery of novel Quinazoline based Thiazolotriazole hybrids as potential EGFR inhibitor: Synthesis, anticancer evaluation and in silico studies

MD Farveen[1], Sudhakar Kalagara[2], E. Balraju[1], B. Jaysree[3], Ayub Shaik[3], Alia Begum[3,*]

[1]*Department of Chemistry, Osmania University, Hyderabad 500007, Telangana, India.* [2]*Department of Chemistry and Biochemistry the University of Texas at EI Paso, EI Paso, TX-79968, USA.* [3]*Department of Chemistry, Telangana Mahila Viswavidyalayam, Koti, Hyderabad, 500095, Telangana, India*

Submitted on: 14-Sep-2024 Accepted and Published on: 18-Nov-2024

Article

ABSTRACT

Significant efforts have been made to design and synthesize novel series of quinazoline based thiazolotriazole analogues (**8a-8n**) and examined for their anticancer activity against two cancer cell lines (MCF-7 & A549). The *in vitro* anticancer activity assessment of these analogues against the EGFR tyrosine kinase revealed that six compounds (**8d**, **8e**, **8f**, **8j**, **8m**, and **8n)** exhibited efficacy against tested cell lines. The results showed that compounds **8d** and **8e** were more active than the standard erlotinib, although compounds **8m** and **8n** were equally effective. *In silico* investigations of the compounds were performed to understand their interactions with the EGFR receptor. The calculated binding energy values of these compounds showed a consistent correlation with their observed IC_{50} values, reinforcing the validity of their predicted efficacy in inhibiting the EGFR kinase. Overall, this study highlighted the potential of the newly prepared analogues as promising leads for further development into anticancer drugs.

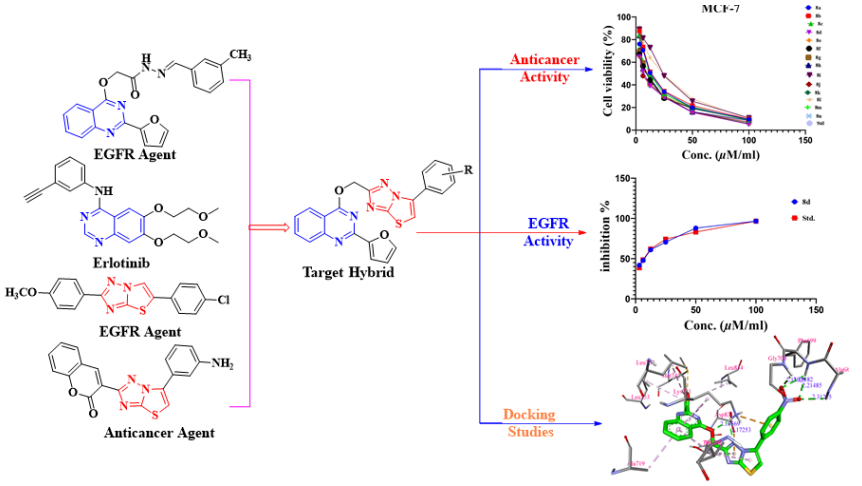

Keywords Quinazoline, Thiazolotriazole, Anticancer, EGFR inhibitor, Molecular docking

INTRODUCTION

The development of potent, selective, and less toxic anticancer agents remains a major challenge in medicinal chemistry. Cancer is among the deadliest diseases in developing countries.[1] The epidermal growth factor receptor (EGFR) is a key target in cancer research due to its critical role in cell survival, proliferation, differentiation, and carcinogenesis. One common mechanism in the progression of cancer, particularly in non-small cell lung cancer (NSCLC), is dysregulation of EGFR. Additionally, overexpression of EGFR has been linked to a variety of malignancies, including those of the breast, head and neck, ovarian, colon, and other tissues.[2] The previously mentioned cancers are treated with EGFR inhibitors, which are FDA-approved drugs like serlotinib,[3] lapatinib,[4] gefitinib,[5] afatinib[6] and icotinib[7] (Figure 1). An important variable in the development of cancer is the interaction between EGFR and reactive oxygen species (ROS).[8] Overexposure to ROS can cause detrimental effects, including cancer cell death or growth inhibition.[9] Mitochondrial dysfunction is also an important mechanism in the induction of oxidative stress. The EGFR downstream survival pathway can be inhibited by higher ROS levels, which can cause the Met residue of EGFR T790M to over oxidize.[10] Consequently, a viable therapeutic strategy for the treatment of cancer may involve either direct EGFR inhibition, inhibition of EGFR activity through enhanced generation of ROS, or both.

The main issue with the current generation of EGFR-inhibiting cancer drugs is side effects. Erlotinib was found to significantly decrease the levels of hemoglobin, red blood cells (RBCs), and white blood cells.[11] In an experimental rat model, it caused internal organ damage and elevated liver function indicators, alanine aminotransferase and aspartate aminotransferase levels.[12] Similarly, in patients with advanced non-small cell lung cancer, erlotinib treatment was associated with uncommon hematologic

*Corresponding Author: Dr. Alia Begum, Department of Chemistry, Telangana Mahila Viswavidyalayam, Koti, Hyderabad-500095, India
Tel: +91 9849170130; Email: alia78ou@gmail.com

URN:NBN:sciencein.cbl.2025.v12.1261
DOI:10.62110/sciencein.cbl.2025.v12.1261

https://pubs.thesciencein.org/cbl

problems.[13] Developing novel EGFR inhibitors as anticancer drugs with minimal damage to normal organs and blood cells is essential.

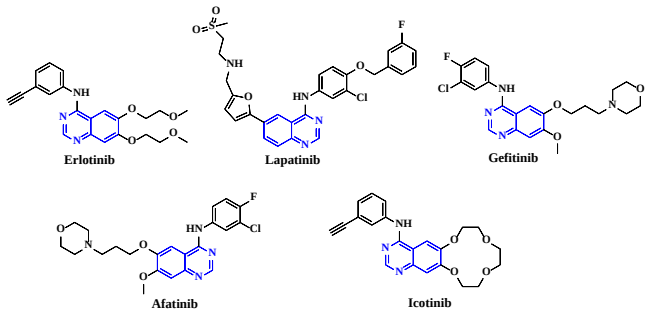

Figure 1. Some reported EGFR inhibitors

The wide range of biological activities of Quinazoline derivatives makes it a valuable heterocyclic moiety in drug discovery and medicinal chemistry.[14] The quinazoline moiety has demonstrated significant activity against various tumor types and has shown to be a crucial contributor to anticancer efficacy in EGFR inhibitors, such as erlotinib and lapatinib. Additionally, the quinazoline core exhibits a range of biological activities, including antibacterial,[15] antifungal,[16] antitubercular,[17] antimalarial,[18] and anticancer properties.[19]

The biological features of fused heterocyclic structures containing nitrogen and sulfur heteroatoms have made them effective scaffolds for study in medicinal chemistry.[20-23] Among these structures, thiazolotriazoles, which combine thiazole and triazole rings, have drawn special attention because of their many applications as antimicrobials,[24] antipyretics,[25] analgesics, anti–inflammatory,[26] anticancer agents,[27] vasodilatory agents,[28] and EGFR inhibitors.[29] Several innovative treatments have been tested, but the majority have significant toxicities. We wanted to create EGFR inhibitors as part of an ongoing research endeavor in our lab to find novel anticancer drugs.[30] A few examples of compounds with a thiazolotriazole core that show a variety of medicinal applications are presented in **Figure 2**.

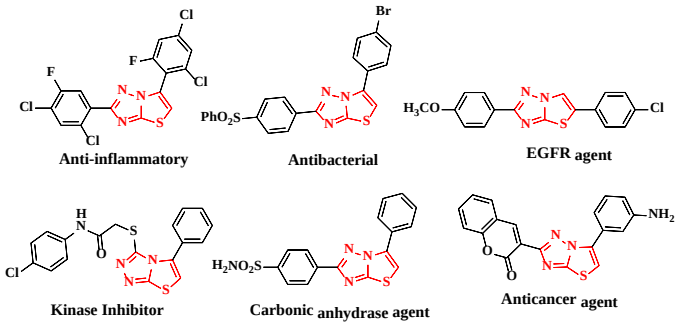

Figure 2. Thiazolotriazole compounds with biological activities

Recently, the design and synthesis of hybrid molecules for the treatment of cancer has led to significant usage of the molecular hybridization strategy. The approach primarily entails integrating two or more pharmacophore moieties into a single molecule with a common scaffold. These hybrid compounds have numerous benefits over conventional pharmaceuticals in terms of solubility, toxicity,[31] resistance to multiple drugs, and other aspects. In this work, we are combining the two scaffolds that are biologically significant, quinazoline and thiazolotriazole, using the molecular hybridization approach to obtain a set of novel hybrid molecules (Figure 3).

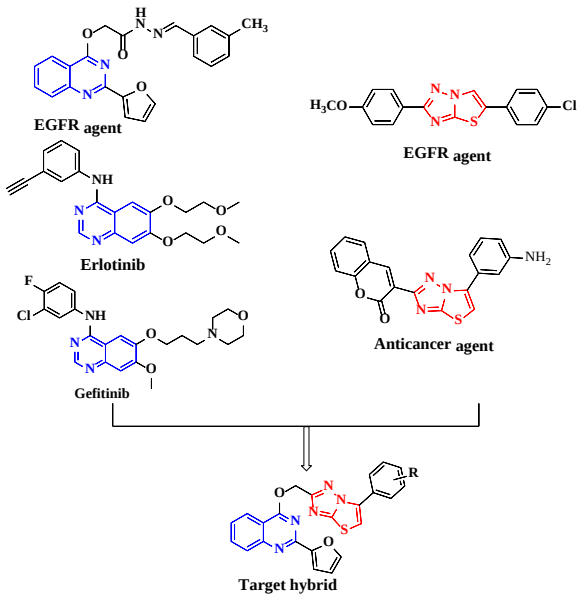

Figure 3. Design strategy of the target hybrid

We synthesized quinazoline based thiazolotriazole hybrid compounds and performed cytotoxicity and molecular docking studies. A lead molecule was used to investigate EGFR inhibition and toxicity in normal cells.

RESULTS AND DISCUSSION

Chemistry

The synthesis of novel quinazoline thiazolotriazole hybrids (**8a-n**) is described in **Scheme 1**. ethyl 2-((2-(furan-2-yl) quinazolin-4-yl)oxy)acetate (**2**) was synthesized starting from 2-(furan-2-yl)quinazolin-4(3*H*)-one (**1**) according to Refs.[32,33] 2-((2-(furan-2-yl)quinazolin-4-yl)oxy)acetohydrazide (**3**) was produced by following Ref. [35] in excellent yield. When compound **3** and potassium thiocyanate were reacted in presence of hydrochloric acid, 2-(2-((2-(furan-2-yl) quinazolin-4-yl)oxy)acetyl)hydrazine-1-carbothioamide (**4**) was produced. Under basic conditions, intramolecular dehydrative cyclization produced the corresponding 5-(((2-(furan-2-yl) quinazolin-4-yl) oxy) methyl)-4*H*-1,2,4-triazole-3-thiol (**5**) in an excellent yield.

Next, the reaction with substituted 2-bromoacetophenones (**6a–n**) produced the corresponding 2-((5-(((2-(furan-2-yl)quinazolin-4-yl)oxy)methyl)-4*H*-1,2,4-triazol-3-yl)thio)-1-substituted phenylethan-1-one (**7a–n**). In the final step, these 2-((5-(((2-(furan-2-yl)quinazolin-4-yl)oxy)methyl)-4*H*-1,2,4-triazol-3-yl)thio)-1- substituted phenylethan-1-ones were cyclized into quinazoline-integrated thiazolotriazoles (**8a–n**) using phosphorus oxychloride. The structural diversity of this hybrid framework originates from the bromoacetophenones, which accommodate a variety of functional groups on the

aromatic ring. The target analogs were successfully synthesized in good yield by incorporating both electron-deficient and electron-rich groups on the ring, as well as through multi-substitution.

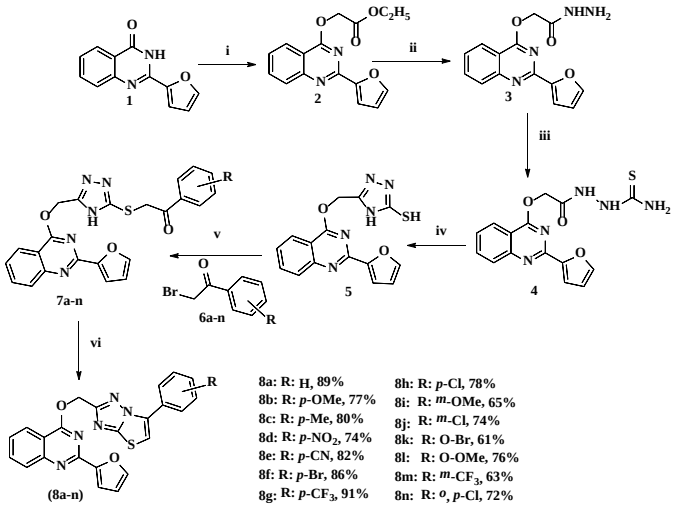

Scheme 1. Reagents and conditions: (**i**) ethyl chloroacetate, K_2CO_3, acetone, reflux, 10 h; (**ii**) hydrazine hydrate, EtOH, reflux, 4 h; (**iii**) KSCN, HCl(aq), reflux, 2h; (**iv**) NaOH(aq), Reflux, 3h; (**v**) KOH, EtOH, reflux, 4-6 h; (**vi**) $POCl_3$, reflux, 4-6 h;

The synthesized quinazoline thiazolotriazole hybrids (**8a-n**) structural elucidation is confirmed by ^{1}H NMR, ^{13}C NMR, and elemental analysis studies in addition to high resolution mass. The ^{1}H NMR spectra of compound **8a** displayed signals: the OCH_2 proton signal at 4.60 ppm, the thiazole ring singlet proton appeared at 8.18 ppm, the furan ring H3, H4 and H5 protons signals displayed at 6.53 ppm, 7.54 ppm and 8.01 ppm and the remaining protons signal appeared at aromatic region. The ^{13}C NMR spectrum of compound **8a** revealed the presence of the OCH_2 carbon signal at 51.89 ppm, the quniazoling-C1 carbon at 180.36 ppm, the quniazoling-C3 carbon at 157.28 ppm, the thaizolotriazole ring-C8 carbon at 176.31 ppm, and the thaizolotriazole ring-C5 carbon at 112.22 ppm, respectively. The ESI-mass spectrum presented the $[M + H]^+$ peak at m/z: 426.03, corresponding to the molecular formula $C_{23}H_{15}N_5O_2S$.

***In vitro* cytotoxic activity**

The *in vitro* cytotoxicity of newly synthesized quinazoline thiazolotriazole hybrids (**8a–8n**) was studied *in vitro* against MCF-7 (human breast cancer) cell lines, A549 (human lung cancer), and MCF-10 A (normal human breast cell) by using the MTT method.[34,35] In this case, erlotinib was used as the control drug, and the results were displayed as the IC_{50} with μM. The survival curves for MCF-7 and A549 were obtained by plotting the relationship between the surviving fraction and drug concentration, as illustrated in **Figure 4**. The cytotoxicity results revealed that the compounds exhibited varying levels of cytotoxic activity against the tested cancer cell lines (**Table 1**). Particularly, compound with 4-nitrophenyl (**8d**) group on the thiazolotriazole ring exhibited better cytotoxic activity than erlotinib against MCF-7 and A549 cell lines with IC_{50} values of 3.70 ± 0.55 μM and 8.45 ± 0.16 μM, respectively, and moreover, compound with 4-cyanophenyl (**8e**) group on the thiazolotriazole ring demonstrated excellent activity against two cell lines with IC_{50} values of 3.75 ± 0.44 μM and 8.56 ± 0.39 μM, respectively. The compounds containing 3-chlorophenyl (**8j**) and 2, 4-dichlorophenyl (**8n**) groups on the thiazolotriazole ring had approximately equipotent activity against the breast cancer cell line (MCF-7) with IC_{50} values of 5.31 ± 0.57 μM, and 5.09 ± 0.51 μM, respectively, compared to erlotinib (MCF-7: IC_{50} = 4.61 ± 0.12 μM). The compounds containing 4-trifloromethylphenyl (**8g**), 3-trifloromethylphenyl (**8m**), and 2, 4-dichlorophenyl (**8n**) groups on the thiazolotriazole ring have displayed good activity against the lung cancer cell line (A549) with IC_{50} values of 10.00 ± 0.91μM, 9.84 ± 0.47 μM and 10.43 ± 0.99μM, respectively, when compared to erlotinib (A549: IC50 = 8.93 ± 0.63 μM), respectively. The remaining compounds **8a**, which contain phenyl, **8b**, which contain 4-methoxylphenyl, **8c**, which contain 4-menthylphenyl, **8f**, which contain 4-bromophenyl, **8h** which contain 4-chlorophenyl, **8i** which contain 3-methoxylphenyl, 2-bromophenyl (**8k**) and 2-methoxylphenyl (**8l**) groups on the thiazolotriazole ring, have shown moderate to poor activity against two tested cell lines (IC_{50} range from 9.13 ± 0.86 μM to 38.58 ± 1.03 μM (MCF-7) and 13.08 ± 0.50 μM to 38.41 ± 1.21 μM (A549), respectively).

Table 1: *In vitro* cytotoxicity of quinazolinethiazolotriazole hybrids (**8a–8n**) with IC_{50} in μM.[a]

Compounds		IC_{50} in μM		
	R	**MCF-7**	**A549**	**MCF-10A**
8a	H	22.63 ± 1.14	20.59 ± 1.13	NT
8b	4-OCH_3	28.40 ± 0.37	31.02 ± 0.73	NT
8c	4-CH_3	24.83 ± 0.69	30. 28 ±0.84	NT
8d	4-NO_2	3.70 ± 0.55	8.45 ± 0.16	16. 03 ±0.14
8e	4-CN	3.75 ± 0.44	8.56 ± 0.39	14.16 ± 0.22
8f	4-Br	9.19 ± 0.90	14.29 ± 0.71	NT
8g	4-CF_3	11.52 ± 1.22	10.00 ± 0.91	14.53 ± 0.09
8h	4-Cl	15.78 ± 1.18	18.92 ± 1.56	NT
8i	3-OCH_3	38.58 ± 1.03	38.41 ± 1.21	NT
8j	3-Cl	5.31 ± 0.57	13.08 ± 0.50	15.60 ± 0.12
8k	2-Br	9.13 ± 0.86	17.67 ± 1.13	NT
8l	2-OCH_3	36.80 ± 0.63	18.83 ± 0.99	NT
8m	3-CF_3	14.57 ± 1.89	9.84 ± 0.47	15.19 ± 0.06
8n	2,4-diCl	5.09 ± 0.51	10.43 ± 0.99	12. 23 ±0.18
Std.	**Erlotinib**	**4.61 ± 0.12**	**8.93 ± 0.63**	**17.08 ± 0.26**

[a]=Values are mean ± SD of three replicates. "NT" =not tested.

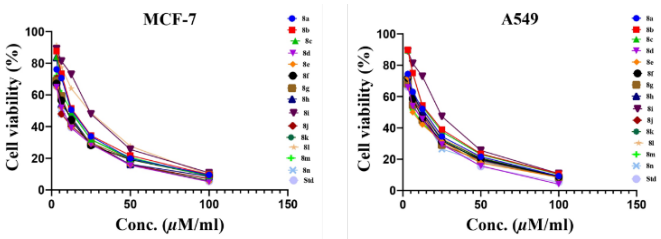

Figure 4. Survival curves of MCF-7 and A549 for quinazoline based thiazolotriazole hybrids (**8a–8n**)

Tyrosine kinase EGFR inhibitory activity

EGFR is known to promote cell migration and invasion of other cells. Thus, it has been demonstrated that these receptors are significant anticancer targets in both breast and non-small cell lung carcinomas. Mutations in EGFR have been discovered in breast tumors that are inherited as well as non-inherited.[36] These days, an EGFR-targeted drug is being investigated as a means of cytotoxically killing breast cancer cells.[37] Many compounds that target tyrosine kinase are being investigated at different stages to potentially be used as EGFR inhibitors.

Table 2: EGFR inhibitory activity of potent compounds.

Compounds	EGFR (IC_{50} μM)*
8d	0.210 ± 0.01
8e	0.318 ± 0.05
8f	0.700 ± 0.04
8j	0.502 ± 0.15
8m	0.828 ± 0.08
8n	0.423 ± 0.01
Erlotinib	0.421 ± 0.03

*Average of triplicates± standard deviation.

An enzymatic assay was used to examine the tyrosine kinase EGFR inhibitory activity of six active hybrids (**8d**, **8e**, **8f**, **8j**, **8m**, and **8n**) based on their cytotoxic properties. **Table 2** findings indicate that **8d** and **8e** were more effective than Erlotinib (IC_{50} = 0.42 ± 0.03 μM), the control drug, and other drugs studied with IC_{50} values of 0.210 ± 0.01 μM and 0.318 ± 0.05 μM in inhibiting EGFR tyrosine kinase. Moreover, compound **8n** has an IC_{50} value of 0.423 ± 0.01 μM and exhibits equipotent inhibition against EGFR. Nevertheless, the compounds **8f**, **8j**, and **8m** have demonstrated good inhibition against EGFR, exhibiting IC_{50} values of 0.700 ± 0.04 μM, 0.502 ± 0.15 μM, and 0.828 ± 0.08 μM as compared with the positive control (**Figure 5**).

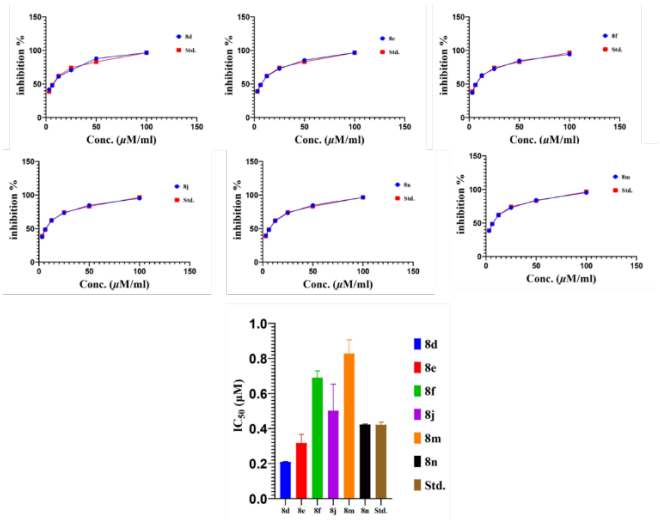

Figure 5. Inhibition% of & *in vitro* IC_{50} (μM) of selected hybrids against EGFR protein kinases.

Molecular docking

The binding mechanism of test compounds with the EGFR enzyme active site was predicted using molecular docking. Notably, the various hybrids (**8d**, **8e**, **8f**, **8j**, **8m**, and **8n**) displayed potent EGFR inhibition in the range from 0.210 ± 0.01 μM to 0.828 ± 0.08 μM. These hybrids were considered to be very strong inhibitors when compared to the reference Erlotinib. All of these hybrids interact with the amino acids present in the active site via their thiazolotriazole group. According to our research, adding nitro and cyano groups to the para position of the phenyl ring could enhance the binding and biological activity of compounds **8d** and **8e**. The molecular docking studies of the synthesized compounds (**8a–8n**) on EGFR revealed that the compounds exhibit hydrogen bonding interactions and binding energies with the target protein, as indicated in **Table 3**.

Table 3: Binding energy and hydrogen bonding interactions of compounds with EGFR kinase enzyme into the active site of 4HJO.

Compds	Binding Energy (kcal/mol)	No. of hydrogen bonds	Residues involved in hydrogen Bonding
8a	-10.82	2	LYS721, ASP831
8b	-10.75	1	ASP831
8c	-10.20	2	LYS721, ASP831
8d	-11.56	6	LYS721 (2), GLY700, PHE699(2), ALA698
8e	-12.23	3	LYS721 (2), ASP831
8f	-11.42	1	ASP831
8g	-10.91	3	LYS721, ASP831, LEU753
8h	-11.36	2	LYS721, ASP831
8i	-11.52	6	LYS721 (4), ASP831, THR830
8j	-11.54	4	LYS721 (3), ASP831
8k	-11.48	3	THR830, ASP831(2)
8l	-10.81	3	LYS721, ASP831(2)
8m	-10.98	5	LYS721, ASP831(2), THR766, CYS773
8n	-11.55	5	LYS721, ASP831 (2), THR766, THR830
Erlotinib	-8.10	1	MET769

The compound **8d** displayed six hydrogen bonds: GLY700, ALA 698, and PHE699 interact with the NO_2 group of oxygen atoms, LYS721 interacts with the OCH_2 group of oxygen atoms, and the triazole ring of nitrogen atoms. The furan ring Pi-cation interaction of MET742, Pi-alkyl interactions of LEU834, 3UE764 and LEU753 residues, quinazoline ring Pi-alkyl interactions of ALA719, VAL702, and LYS721 amino acids, thiazolotriazole ring Pi-alkyl interaction of VAL702 and Pi-Cation interact with ASP831 and phenyl ring pi-cation interaction of LY721 amino acid, as displayed in **Figure 6**. The compound **8e** exhibited three hydrogen bonds: LYS721 interacts with the -OCH_2 group of the oxygen atom and the triazole ring of the nitrogen atom, and ASP831 interact with the triazole ring of the nitrogen atom. The furan ring pi-alkyl interactions of ALA719 and MET769 amino acids and pi-sigma interaction of LEU820 amino acid; the quinazoline ring pi-sigma interactions of VAL702 and LEU820, the thiazolotriazole ring pi-alkyl

interacts with LEU764, LEU834, and LYS721 amino acids and the pi-anion interacts with ASP831 amino acid; and the phenyl ring pi-alkyl interaction of MET742 and LEU753 amino acids, as shown in **Figure 7**. The compounds **8j** and **8n** exhibit hydrogen bonds four with the LYS721 (3) and ASP831 amino acids (**8j**) and five hydrogen bonds with the LYS721, ASP831 (2), THR766, and THR830 amino acids (**8n**), respectively. The remaining pi-sigma, pi-sulfur, halogen, pi-alkyl and alkyl interactions are displayed in **Figures 8** & **9**.

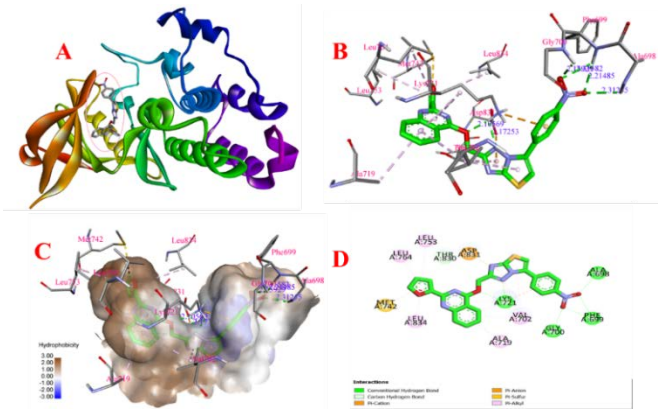

Figure 6. The binding mode of compound **8d** in the active site of EGFR (A) orientation of ligand with protein, (B) 3D interactions, (C) Hydrophobic surface interactions, (D) 2D interactions

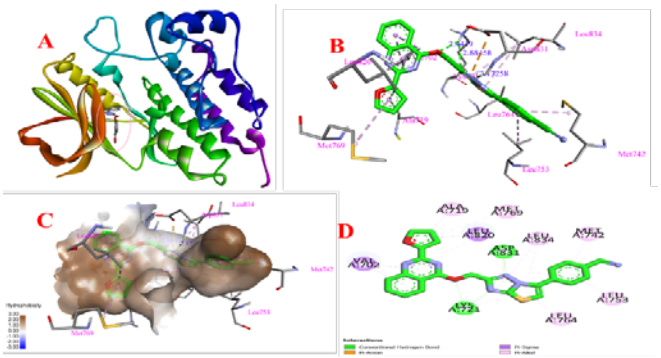

Figure 7. The binding mode of compound **8e** in the active site of EGFR (A) orientation of ligand with protein, (B) 3D interactions, (C) Hydrophobic surface interactions, (D) 2D interactions

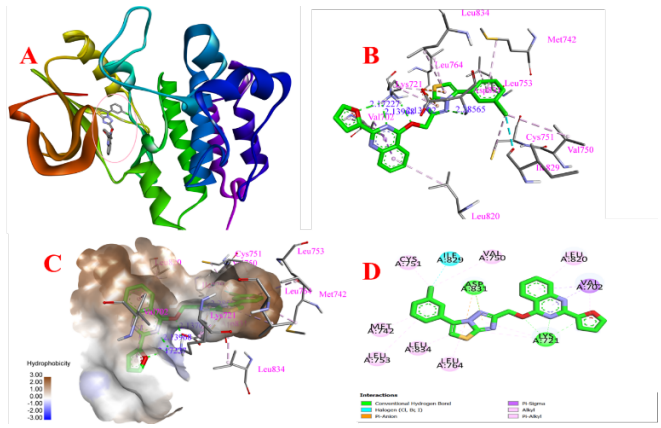

Figure 8. The binding mode of compound **8j** in the active site of EGFR (A) orientation of ligand with protein, (B) 3D interactions, (C) Hydrophobic surface interactions, (D) 2D interactions

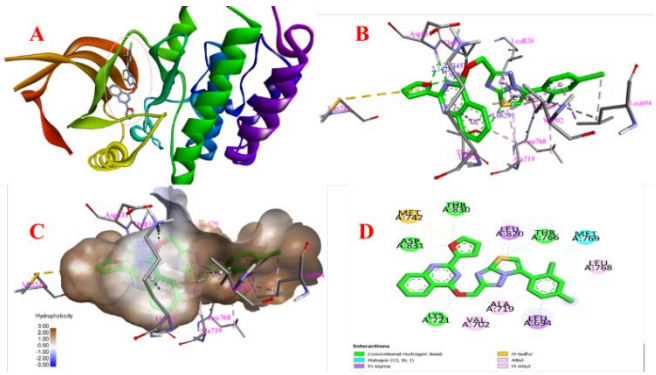

Figure 9. The binding mode of compound **8n** in the active site of EGFR (A) orientation of ligand with protein, (B) 3D interactions, (C) Hydrophobic surface interactions, (D) 2D interactions

Experimental Section

Materials and Methods:

All the reagents were of analytical grade or chemically pure. Analytical TLC was performed on silica gel 60 F254 plates. ^{1}H-NMR spectra were recorded on a Varian Gemini 400 MHz spectrometer by using tetramethyl silane as an internal standard. ^{13}C-NMR spectra were recorded on a Bruker 100 MHz spectrometer. Mass spectral measurements were conducted using EI method. Elemental analyses were performed on a Carlo Erba 106 and Perkin-Elmer Model 240 analyzers. The melting points were measured with a Cintex apparatus and were not corrected.

Ethyl 2-((2-(furan-2-yl)quinazolin-4-yl)oxy)acetate (2):

The mixture of 2-(furan-2-yl)quinazolin-4(3H)-one (**1**) (10 mmol), ethyl chloroacetate (12.5 mmol), and anhydrous potassium carbonate (1.25 g) was refluxed in dry acetone (25 mL) for 10 h. After heating, the reaction mixture was filtered. Once cooled, the filtrate was poured over crushed ice and filtered again, obtaining a yield of 83%.

2-((2-(furan-2-yl)quinazolin-4-yl)oxy)acetohydrazide (3):

A mixture of compound **2** (10 mmol) with hydrazine hydrate (20 mmol) in 20 mL of ethanol was refluxed for 4 h. The reaction mixture was concentrated, allowed to cool, filtered, and crystallized in methanol, obtaining a yield of 79%.

2-(2-((2-(furan-2-yl)quinazolin-4-yl)oxy)acetyl)hydrazine-1-carbothioamide (4):

A mixture of 2-((2-(furan-2-yl)quinazolin-4-yl)oxy)acetohydrazide(**3**) (10 mmol) and potassium thiocyanate (10 mmol) was added to 5 mL of an aqueous HCl solution. The reaction mixture was refluxed for 2 h. After cooling, the mixture was poured over cursed ice. Following filtering, drying, and recrystallization with ethanol, the resultant solid was obtained, resulting in a yield of 81%.

5-(((2-(furan-2-yl)quinazolin-4-yl)oxy)methyl)-4H-1,2,4-triazole-3-thiol (5):

Compound **4** (10 mmol) was added to 100 cm^{3} of a 5% NaOH solution and refluxed for 3h. The reaction mixture was cooled, poured onto crushed ice and neutralized with a concentrated HCl solution. The product obtained was dried and recrystallized from a mixture of ethanol and dimethylformamide, resulting in a yield of 74%.

General procedure for the preparation of 2-((5-(((2-(furan-2-yl)quinazolin-4-yl)oxy)methyl)-4H-1,2,4-triazol-3-yl)thio)-1-substituted phenylethan-1-one (7a-n):

Compound **5** (10 mmol) was added to substituted phenacyl bromides (**6a-n**) together with KOH (15 mmol) in absolute ethanol, and the mixture was refluxed for 4-6 hours. The reaction mixture is chilled and streamed onto crushed ice. The precipitate was collected, and the crude product was purified using silica gel chromatography with an eluent (25% ethyl acetate in hexane). The yields of compounds (**7a-n**) were between 65 and 90%.

General procedure for the preparation of 2-(((2-(furan-2-yl)quinazolin-4-yl)oxy)methyl)-6- substituted phenylthiazolo[3,2-b][1,2,4]triazole (8a-n):

To 10 mmol of 2-((5-(((2-(furan-2-yl)quinazolin-4-yl)oxy)methyl)-4H-1,2,4-triazol-3-yl)thio)-1- substituted phenylethan-1-one (**7**), 5 mL of $POCl_3$ was added and refluxed for 4-6 h. The reaction mixture was cooled, poured into ice water and neutralized with sodium bicarbonate .The resulting solid was filtered, dried, and recrystallized using a mixture of ethanol and dimethylformamide.

2-(((2-(furan-2-yl)quinazolin-4-yl)oxy)methyl)-6-phenylthiazolo[3,2-b][1,2,4]triazole (8a):

Light Yellow solid; Yield 89%; m.p: 254-256 ˚C; ^{1}H NMR (400 MHz, DMSO-d_6): δ 8.18 (s, 1H, thiazol-H), 8.08 (dd, J = 7.6, 1.4 Hz, 1H, Ar-H), 8.01 (dd, J = 7.6, 1.4 Hz, 1H, Ar-H), 7.94 (dd, J = 7.6, 1.4 Hz, 1H, Ar-H), 7.82 – 7.72 (m, 4H, Ar-H), 7.60 – 7.54 (m, 1H, Ar-H), 7.48 (t, J = 7.4 Hz, 2H, Ar-H), 7.43 – 7.36 (m, 1H, Ar-H), 6.53 (t, J = 7.6 Hz, 1H, Ar-H), 4.60 (s, 2H, OCH_2); ^{13}C NMR (100 MHz,DMSO-d_6): δ 180.36, 176.31, 157.28, 157.20, 154.32, 145.04, 143.77, 140.66, 133.36, 130.99, 129.57, 128.82, 128.69, 127.21, 126.94, 124.77, 117.15, 113.35, 112.22, 108.29, 51.89; ESI-MS: m/z 426 $[M+H]^+$; $C_{23}H_{15}N_5O_2S$; Calculated, %: C, 64.93; H, 3.55; N, 16.46; Found, %: C, 64.89; H, 3.63; N, 16.38.

2-(((2-(furan-2-yl)quinazolin-4-yl)oxy)methyl)-6-(4-methoxyphenyl)thiazolo[3,2-b][1,2,4]triazole (8b):

Pale yellow solid; yield 77 % m.p. 260-262 ˚C; ^{1}H NMR (400 MHz, DMSO-d_6): δ 8.11 (dd, *J* = 7.4, 1.2 Hz, 2H), 7.94 (dd, *J* = 7.4, 1.2 Hz, 1H), 7.79 (td, *J* = 7.6, 1.4 Hz, 1H), 7.73 (d, *J* = 7.4 Hz, 2H), 7.64 (dd, *J* = 7.6, 1.4 Hz, 1H), 7.63 (s, 1H), 7.56 (td, *J* = 7.4, 1.2 Hz, 1H), 7.10 (d, *J* = 7.4 Hz, 2H), 6.90 (t, *J* = 7.4 Hz, 1H), 5.53 (s, 2H), 3.80 (s, 3H); ^{13}C NMR (100 MHz, DMSO-d_6) δ 176.31, 168.36, 158.96, 157.28, 157.20, 154.32, 145.04, 143.77, 140.66, 133.36, 128.69, 128.21, 126.94, 124.76, 124.61, 117.15, 115.09, 113.35, 112.22, 108.29, 56.03, 51.89; ESI-MS: m/z 456 $[M+H]^+$; $C_{23}H_{15}N_5O_2S$; Calculated, %: C, 63..29; H, 3.73; N, 15.38; Found, %: C, 63.32; H, 3.69; N, 15.45.

2-(((2-(furan-2-yl)quinazolin-4-yl)oxy)methyl)-6-(p-tolyl)thiazolo[3,2-b][1,2,4]triazole (8c):

Yellow solid; yield 80%; m.p. 282-284 ˚C; ^{1}H NMR (400 MHz, DMSO-d6): δ 8.12 (dd, *J* = 7.5, 1.2 Hz, 1H, furan-H5), 8.08 (dd, *J* = 7.5, 1.2 Hz, 1H, Ar-H), 7.96 (dd, *J* = 7.4, 1.4 Hz, 1H, Ar-H), 7.82 (td, *J* = 7.5, 1.4 Hz, 1H, Ar-H), 7.70 (d, *J* = 7.5 Hz, 2H, Ar-H), 7.66 – 7.63 (m, 1H, Ar-H), 7.63 (S, 1H, thiazole-H), 7.58 (td, *J* = 7.5, 1.4 Hz, 1H, Ar-H), 7.36 (d, *J* = 7.5 Hz, 2H, Ar-H), 6.92 (t, *J* = 7.5 Hz, 1H, Ar-H), 5.63 (s, 2H, -OCH_2), 2.38 (s, 3H, -CH_3); (100 MHz, DMSO-d_6): δ 176.34, 168.33, 157.23, 157.22, 154.35, 145.01, 143.79, 140.69, 138.33, 133.33, 130.51, 129.62, 128.71, 127.70, 126.96, 124.79, 117.15, 113.38, 112.25, 108.32, 51.92, 21.52; ESI-MS: m/z 440 $[M+H]^+$; $C_{24}H_{17}N_5O_2S$; Calculated, %: C, 65.59; H, 3.90; N, 15.94; Found, %: C, 65.54; H, 3.71; N, 15.99.

2-(((2-(furan-2-yl)quinazolin-4-yl)oxy)methyl)-6-(4-nitrophenyl)thiazolo[3,2-b][1,2,4]triazole (8d):

Pale yellow solid; yield 74%; m. p. 274-276 ˚C; ^{1}H NMR (400 MHz, DMSO-d_6): δ 8.40 (d, J = 7.7 Hz, 2H, Ar-H), 8.18 (s, 1H, Thiazole-H), 8.07 (dd, J = 7.5, 1.5 Hz, 1H, Ar-H), 8.03 (d, J = 7.7 Hz, 3H, furan-H5 and Ar-H), 8.00 (dd, J = 7.4, 1.6 Hz, 1H, Furan-H3), 7.94 (dd, J = 7.6, 1.4 Hz, 1H), 7.78 (td, J = 7.4, 1.2 Hz, 1H, Ar-H), 7.56 (td, J = 7.8, 1.6 Hz, 1H, Ar-H), 7.04 (t, J = 7.6 Hz, 1H, Furan-H4), 5.69 (s, 2H, -OCH_2); ^{13}C NMR (100 MHz, DMSO-d_6): δ 176.31, 168.38, 157.28, 157.23, 154.30, 147.50, 145.07, 143.73, 140.68, 135.61, 133.36, 128.66, 127.06, 126.99, 125.07, 124.73, 117.16, 113.32, 112.28, 108.28, 51.88; ESI-MS: m/z 470 $[M]^+$; $C_{23}H_{14}N_6O_4S$; Calculated, %: C, 58.72; H, 3.00; N, 17.86; Found, %: C, 58.76; H, 2.97; N, 17.81.

4-(2-(((2-(furan-2-yl)quinazolin-4-yl)oxy)methyl) thiazolo[3,2-b][1,2,4]triazol-6-yl)benzonitrile (8e):

Light orange solid; yield 82 %; m.p. 284-286 ˚C; ^{1}H NMR (400 MHz, DMSO-d_6): δ 8.18 (s, 1H, Thiazole-H), 8.09 (dd, *J* = 7.6, 1.4 Hz, 1H, Ar-H), 8.03 (dd, *J* = 7.4, 1.2 Hz, 1H, Ar-H), 7.94 (dd, *J* = 11.6, 4.5 Hz, 3H, Ar-H), 7.82 – 7.76 (m, 1H, Ar-H), 7.76 – 7.70 (m, 3H, Ar-H), 7.57 (td, *J* = 7.4, 1.4 Hz, 1H, Ar-H), 6.50 (t, *J* = 7.6 Hz, 1H, Ar-H), 5.65 (s, 2H, -OCH_2); (100 MHz, DMSO-d_6): δ 176.38, 168.34, 157.31, 157.25, 154.35, 145.06, 143.74, 140.62, 133.38, 131.39, 131.01, 130.45, 128.71, 126.96, 124.72, 119.15, 117.16, 113.38, 112.83, 112.24, 108.22, 52.03; ESI-MS: m/z 451 $[M+H]^+$; $C_{24}H_{14}N_6O_2S$; Calculated, %: C, 63.99; H, 3.13; N, 18.66; Found, %: C, 63.96; H, 3.18; N, 18.61.

6-(4-bromophenyl)-2-(((2-(furan-2-yl)quinazolin-4-yl)oxy)methyl)thiazolo[3,2-b][1,2,4]triazole (8f)

Yellow solid; yield 86%; m.p. 214-216 ˚C; ^{1}H NMR (400 MHz, DMSO-d_6): δ 8.10 (dd, *J* = 7.6, 1.4 Hz, 1H, Ar-H), 8.05 (dd, *J* = 7.6, 1.4 Hz, 1H, Ar-H), 7.97 (dd, *J* = 7.6, 1.4 Hz, 1H, Ar-H), 7.81 (dd, *J* = 9.0,1.2 Hz, 2H, Ar-H), 7.63 (s, 1H, Thiazole-H), 7.60 (dd, *J* = 7.6, 1.4 Hz, 1H, Ar-H), 7.57 (dd, *J* = 7.1, 4.5 Hz, 2H, Ar-H), 7.46 (d, *J* = 7.4 Hz, 2H, Ar-H), 6.81 (t, *J* = 7.4 Hz, 1H, Ar-H), 5.76 (s, 2H, -OCH_2); ^{13}C NMR (100 MHz, DMSO-d_6): δ 176.28, 168.37, 157.30, 157.24, 154.35, 145.02, 143.78, 140.64, 133.39, 132.41, 128.72, 128.29, 127.52, 126.92, 124.76, 123.56, 117.21, 113.39, 112.26, 108.29, 51.93;ESI-MS: m/z 505 $[M+2]^+$; $C_{23}H_{14}N_5BrO_2S$; Calculated, %: C, 54.77; H, 2.80; N, 13.89; Found, %: C, 54.81; H, 2.75; N, 13.92.

2-(((2-(furan-2-yl)quinazolin-4-yl)oxy)methyl)-6-(4-(trifluoromethyl)phenyl)thiazolo[3,2-b][1,2,4]triazole (8g):

Light brown solid; yield 91%; m.p. 262-264 ˚C; ^{1}H NMR (400 MHz, DMSO-d_6): δ 8.10 – 8.07 (m, 2H, Ar-H), 7.96 (dd, *J* = 7.4, 1.2 Hz, 1H, Ar-H), 7.80 (td, *J* = 7.4, 1.4 Hz, 1H, Ar-H), 7.65 (dd, *J* = 11.9, 7.4 Hz, 4H, Ar-H), 7.63 (s, 1H, Thiazole-H), 7.58 (td, *J* = 7.4, 1.4 Hz, 1H, Ar-H), 7.48 (dd, *J* = 7.6, 1.4 Hz, 1H, Ar-H), 6.69 (t, *J* = 7.6 Hz, 1H, Ar-H), 5.64 (s, 2H, -OCH_2); ^{13}C NMR (100 MHz, DMSO-d_6): δ 176.38, 168.39, 157.28, 154.32, 145.04,

143.76, 140.63, 136.70, 133.36, 132.29, 128.83, 128.69, 127.68, 126.94, 125.51, 124.77, 123.41, 121.36, 117.18, 113.35, 112.25, 108.29, 51.92; ESI-MS: m/z 494 $[M+H]^+$; $C_{24}H_{14}F_3N_5O_2S$; Calculated, %: C, 58.42; H, 2.86; N, 14.19; Found, %: C, 58.39; H, 2.81; N, 14.25.

6-(4-chlorophenyl)-2-(((2-(furan-2-yl)quinazolin-4-yl)oxy)methyl)thiazolo[3,2-b][1,2,4]triazole (8h):

Pale yellow solid; yield 78 %; m.p. 260-262 ˚C; ^{1}H NMR (400 MHz, DMSO-d_6): δ 8.10 (dd, *J* = 7.4, 1.2 Hz, 1H, Ar-H), 8.05 (dd, *J* = 7.6, 1.4 Hz, 1H, Ar-H), 7.97 (dd, *J* = 7.6, 1.4 Hz, 1H, Ar-H), 7.84 – 7.79 (m, 2H, Ar-H), 7.66 (s, 1H, Thiazole-H), 7.59 (td, *J* = 7.6, 1.4 Hz, 1H, Ar-H), 7.51 (d, *J* = 7.7 Hz, 2H, Ar-H), 7.41 (d, *J* = 7.3 Hz, 2H, Ar-H), 6.81 (t, *J* = 7.6 Hz, 1H, Ar-H), 5.65 (s, 2H, -OCH_2); ^{13}C NMR (100 MHz, DMSO-d_6): δ 176.33, 168.34, 157.32, 154.35, 145.08, 143.74, 140.62, 135.18, 133.34, 132.23, 129.24, 128.68, 126.95, 124.79, 117.17, 113.39, 112.21, 108.36, 51.99; ESI-MS: m/z 460 $[M+H]^+$; $C_{23}H_{14}ClN_5O_2S$; Calculated, %: C, 60.07; H, 3.07; N, 15.23; Found, %: C, 60.11; H, 3.02; N, 15.28.

2-(((2-(furan-2-yl)quinazolin-4-yl)oxy)methyl)-6-(3-methoxyphenyl)thiazolo[3,2-b][1,2,4]triazole (8i):

White solid; yield 65%; m.p. 274-276 ˚C; ^{1}H NMR (400 MHz, DMSO-d_6): δ 8.08 (ddd, *J* = 13.5, 7.8, 1.6 Hz, 2H, Ar-H), 7.94 (dd, *J* = 7.6, 1.4 Hz, 1H, Ar-H), 7.79 (td, *J* = 7.6, 1.4 Hz, 1H, Ar-H), 7.62 (s, 1H, Thiazole-H), 7.61 (dd, *J* = 7.6, 1.4 Hz, 1H, Ar-H), 7.56 (td, *J* = 7.6, 1.4 Hz, 1H, Ar-H), 7.42 (dd, *J* = 10.2, 4.5 Hz, 2H, Ar-H), 7.32 (dt, *J* = 7.4, 1.4 Hz, 1H, Ar-H), 7.00 – 6.96 (m, 1H, Ar-H), 6.71 (t, *J* = 7.6 Hz, 1H, Ar-H), 5.66 (s, 2H, -OCH_2), 3.78 (s, 3H, OCH_3); ^{13}C NMR (100 MHz, DMSO-d_6): δ 176.38, 168.32, 161.42, 157.22, 154.32, 145.06, 143.79, 139.79, 133.38, 133.01, 129.74, 128.72, 126.99, 124.74, 120.19, 117.12, 115.58, 114.62, 113.38, 112.64, 108.35, 53.09, 52.06; ESI-MS: m/z 455 $[M+H]^+$; $C_{24}H_{17}N_5O_3S$; Calculated, %: C, 63.29; H, 3.76; N, 15.38; Found, %: C, 63.26; H, 3.81; N, 15.42.

6-(3-chlorophenyl)-2-(((2-(furan-2-yl)quinazolin-4-yl)oxy)methyl)thiazolo[3,2-b][1,2,4]triazole (8j):

Pale yellow solid; yield 74%; m.p. 282-284 ˚C; ^{1}H NMR (400 MHz, DMSO-d_6): δ 8.18 (s, 1H, thiazole-H), 8.08 (dd, *J* = 7.6, 1.4 Hz, 1H, Ar-H), 8.02 (dd, *J* = 7.6, 1.4 Hz, 1H, Ar-H), 7.95 (dd, *J* = 7.6, 1.4 Hz, 1H, Ar-H), 7.92 (s, 1H, Ar-H), 7.81 – 7.75 (m, 2H, Ar-H), 7.59 – 7.55 (m, 2H, Ar-H), 7.41 (d, *J* = 4.7 Hz, 2H, Ar-H), 6.51 (t, *J* = 7.6 Hz, 1H, Ar-H), 5.69 (s, 2H, -OCH_2); ^{13}C NMR (100 MHz, DMSO-d_6): δ 176.39, 168.40, 157.26, 154.35, 145.01, 143.78, 139.81, 134.72, 133.63, 133.38, 129.87, 128.73, 127.61, 126.98, 126.43, 126.12, 124.79, 117.18, 113.39, 112.66, 108.31, 51.96; ESI-MS: m/z 461 $[M+H]^+$; $C_{24}H_{17}N_5O_3S$; Calculated, %: C, 60.07; H, 3.07; N, 15.23; Found, %: C, 60.11; H, 3.04; N, 15.28.

6-(2-bromophenyl)-2-(((2-(furan-2-yl)quinazolin-4-yl)oxy)methyl)thiazolo[3,2-b][1,2,4]triazole (8k):

Light yellow solid; yield 61%; m.p. 276-278 ˚C; ^{1}H NMR (400 MHz, DMSO-d_6): δ 8.07 (ddd, *J* = 7.5, 6.1, 1.2 Hz, 2H, Ar-H), 8.03 (dd, *J* = 7.6, 1.4 Hz, 1H, Ar-H), 7.92 (dd, *J* = 7.4, 1.2 Hz, 1H, Ar-H), 7.79 (td, *J* = 7.4, 1.2 Hz, 1H, Ar-H), 7.63 (s, 1H, thiazole-H), 7.60 – 7.53 (m, 3H, Ar-H), 7.39 (td, *J* = 7.6, 1.4 Hz, 1H, Ar-H), 7.24 (td, *J* = 7.4, 1.4 Hz, 1H, Ar-H), 6.83 (t, *J* = 7.6 Hz, 1H, Ar-H), 5.56 (s, 2H, -OCH_2); ^{13}C NMR (100 MHz, DMSO-d_6): δ 176.34, 168.33, 157.21, 154.35, 145.01, 143.73, 140.37, 133.38, 132.51, 131.35, 130.10, 128.72, 128.08, 126.93, 124.74, 122.18, 117.13, 113.39, 109.38, 108.26, 51.96; ESI-MS: m/z 503 $[M]^+$; $C_{23}H_{14}BrN_5O_2S$; Calculated, %: C, 54.77; H, 2.80; N, 13.89; Found, %: C, 54.73; H, 2.86; N, 13.85.

2-(((2-(furan-2-yl)quinazolin-4-yl)oxy)methyl)-6-(2-methoxyphenyl)thiazolo[3,2-b][1,2,4]triazole (8l):

White solid; yield 61%; m.p. 264-266 ˚C; ^{1}H NMR (400 MHz, DMSO-d_6): δ 8.29 (dd, *J* = 7.6, 1.4 Hz, 1H, Ar-H), 8.18 (s, 1H, Thiazole-H), 8.05 (dd, *J* = 7.6, 1.4 Hz, 1H, Ar-H), 7.91 (dd, *J* = 7.6, 1.4 Hz, 1H, Ar-H), 7.77 (td, *J* = 7.4, 1.4 Hz, 1H, Ar-H), 7.69 (dd, *J* = 7.4, 1.6 Hz, 1H, Ar-H), 7.59 – 7.46 (m, 2H, Ar-H), 7.33 (td, *J* = 7.6, 1.4 Hz, 1H, Ar-H), 7.17 – 7.04 (m, 2H, Ar-H), 6.76 (t, *J* = 7.4 Hz, 1H, Ar-H), 5.62 (s, 2H, -OCH_2), 3.76 (s, 3H, -OCH_3); ^{13}C NMR (100 MHz, DMSO-d_6): δ 176.34, 168.35, 159.89, 157.18, 154.35, 145.08, 143.72, 133.33, 130.43, 129.37, 128.74, 126.96, 124.75, 121.86, 121.44, 117.19, 116.45, 113.32, 108.35, 103.03, 53.08, 51.96; ESI-MS: m/z 456 $[M]^+$; $C_{24}H_{17}N_5O_3S$; Calculated, %: C, 63.29; H, 3.76; N, 15.38; Found, %: C, 63.33; H, 3.81; N, 15.26.

2-(((2-(furan-2-yl)quinazolin-4-yl)oxy)methyl)-6-(3-(trifluoromethyl)phenyl)thiazolo[3,2-b][1,2,4]triazole (8m):

Light yellow solid; yield 63%; m.p. 272-274 ˚C; ^{1}H NMR (400 MHz, DMSO-d_6): δ 8.51 (dd, *J* = 7.4, 1.2 Hz, 1H, Ar-H), 8.19 (s, 1H, Ar-H), 8.07 (dd, *J* = 7.4, 1.2 Hz, 1H, Ar-H), 7.95 (dd, *J* = 7.4, 1.6 Hz, 1H, Ar-H), 7.79 (td, *J* = 7.4, 1.4 Hz, 1H, Ar-H), 7.71 (dt, *J* = 7.4, 1.4 Hz, 1H, Ar-H), 7.65 (s, 1H, Thiazole-H), 7.61 – 7.54 (m, 2H, Ar-H), 7.46 (dt, *J* = 15.1, 6.9 Hz, 2H, Ar-H), 6.70 (t, *J* = 7.6 Hz, 1H, Ar-H), 5.60 (s, 2H, -OCH_2); ^{13}C NMR (100 MHz, DMSO-d_6): δ 176.38, 168.35, 157.24, 154.36, 145.01, 143.79, 139.74, 133.31, 132.23, 132.06, 131.01, 129.58, 128.66, 127.24, 126.96, 125.11, 124.79, 124.09, 123.09, 121.00, 117.17, 113.38, 112.66, 108.32, 51.98; ESI-MS: m/z 494 $[M+H]^+$; $C_{24}H_{14}F_3N_5O_2S$; Calculated, %: C, 58.42; H, 2.86; N, 14.19; Found, %: C, 58.47; H, 2.81; N, 14.25.

6-(2,4-dichlorophenyl)-2-(((2-(furan-2-yl)quinazolin-4-yl)oxy)methyl)thiazolo[3,2-b][1,2,4]triazole (8n):

White solid; yield 72%; m.p. 240-242 ˚C; ^{1}H NMR (400 MHz, DMSO-d_6): δ 8.08 (ddd, *J* = 13.8, 7.6, 1.4 Hz, 2H, Ar-H), 7.91 (ddd, *J* = 7.6, 5.1, 1.6 Hz, 2H, Ar-H), 7.79 (td, *J* = 7.4, 1.2 Hz, 1H, Ar-H), 7.64 (s, 1H, thiazole-H), 7.58 (d, *J* = 7.4 Hz, 1H, Ar-H), 7.55 (td, *J* = 7.5, 1.4 Hz, 1H, ArH), 7.50 (s, 1H, Ar-H), 7.36 (d, *J* = 9.0 Hz, 1H, Ar-H), 6.83 (t, *J* = 7.6 Hz, 1H, Ar-H), 5.54 (s, 2H, -OCH_2); ^{13}C NMR (100 MHz, DMSO-d_6): δ 176.35, 168.39, 157.26, 157.22, 154.30, 145.05, 143.78, 135.18, 133.34, 132.95, 131.19, 130.25, 128.65, 127.61, 126.96, 124.79, 117.12, 113.33, 108.32, 51.96;ESI-MS: m/z 495 $[M+2]^+$; $C_{23}H_{13}Cl_2N_5O_2S$; Calculated, %: C, 55.88; H, 2.65; N, 14.17; Found, %: C, 55.85; H, 2.70; N, 14.22.

***In vitro* anticancer activity**

The MTT-micro cultured tetrazolium assay was used for determining cell viability in the presence of the test samples. This assay is a quantitative colorimetric method for the determination of cell viability. The assessed parameter is the metabolic activity of viable cells. Metabolically active cells reduce pale yellow

tetrazolium salt (MTT) to a dark blue water-insoluble formazan, which can be directly quantified after solubilization with DMSO. The absorbance of the formazan directly correlates with the number of viable cells. MCF-7, A549, and MCF-10A cells were plated into a 96-well plate at a 1×10^4 cells/well density. Cells were grown overnight in the entire medium and then switched to the low serum media. 1% DMSO was used as a control. After 48 h of treatment with different concentrations of test compounds, the cells were incubated with MTT (2.5 mg/mL) in the CO_2 chamber for 2 h. The medium was then removed, and 100 μL of DMSO was added to each well to dissolve formazan crystals. After thoroughly mixing, the plates were read at 570 nm for optical density, which is directly correlated with cell quantity. The results were represented as the percentage of viability. All the experiments were carried out in triplicate. The IC_{50} values were calculated using linear regression analysis from the graph pad prism (5.02 version) (P values are significant <0.001). The response parameter is calculated as the IC_{50} value, which corresponds to the concentration required for 50% inhibition of cell viability.

EGFR kinase inhibitory assay

The inhibition of the tyrosine kinase EGFR was assessed using the EGFR Kinase Assay Kit (PBS Bioscience, catalog #40321). Erlotinib served as the standard reference. The results of all the seven compounds were in triplicates. The average of the three experiments and the standard deviation of the three experiments are used to compute the IC_{50} value of the compounds and the reference.

Molecular docking.

To explain the interactive mechanism of quinazoline thiazolotriazole hybrids with most binding sites of receptors, a molecular docking protocol has been used. ChemBioDraw Ultra 12.0 software was used to generate the 2D structures of all the compounds. The crystallographic 3D structure of EGFR protein was extracted from the RCSB Protein Data Bank (www.rscb.org) with PDB ID: 4HJO, respectively. The downloaded proteins' formerly associated ligands and water molecules were removed using the UCSF chimera 1.10.1 program, followed by geometry optimization. The molecular docking studies were carried out using AutoDock Tools (ADT) version 1.5.6 and the AutoDock 4.2 package suite. The docking process was performed between the rigid protein receptor EGFR and the flexible quinazoline thiazolotriazole analogues. The non-polar hydrogens were merged into related carbon atoms of the receptor EGFR using the AutoDock Tools 1.5.6 software. Non-polar hydrogens, Gasteiger charges, and torsion degrees of freedom were also assigned by the AutoDock Tools 1.5.6 program. The distance between donor and acceptor atoms showing the hydrogen bonding interactions was fixed to be 1.9 Å. Moreover, 10 docked conformations were generated for each analogue during the docking protocol, and their structures were saved in PDBQT format. The energy calculations were done by using genetic algorithms. Docking simulations were carried out using grid resolutions. In this docking protocol, a population size of 150, and the maximum number of evaluations, 2.5×10^6 were used to optimize the binding mode of ligands. The output results were graphically analyzed by Discovery Studio 4.1.0.[38]

CONCLUSION

In order to develop a novel family of EGFR inhibitors, we have successfully proven the synthesis of a new hybrid skeleton combining quinazoline and thiazolotriazole compounds. An easy and straight forward synthetic approach obtained the desired hybrids (**8a-8n**) in good yields. We examined the newly prepared analogues for their anticancer activity against MCF-7 and A549. Among all the examined compounds, some of the analogues **8d**, **8e**, **8f**, **8j**, **8m**, and **8n**) active against MCF-7. Selectively, compounds **8d** and **8e** were shown to be more potent with IC_{50} values of 3.70 ± 0.55 μM, and 3.75 ± 0.44 μM against MCF-7 as compared to standard Erlotinib (4.61 ± 0.12 μM). The results of the tyrosine kinase EGFR inhibitory activity of potent compounds **8d**, **8e**, **8f**, **8j**, **8m**, and **8n** revealed that compounds **8d** and **8e** were more effective than the positive control erlotinib (0.421 ± 0.03 μM), with IC_{50} values of 0.210 ±0.01 μM and 0.318 ± 0.05 μM, respectively. Remarkably, *in silico* analyses, including molecular docking of compounds (**8a–8n**), demonstrated consistency with the corresponding *in vitro* activity IC_{50} data.

ACKNOWLEDGMENTS

The authors are grateful to the Indian Institute of Chemical Technology (CSIR-IICT), Hyderabad, for providing the NMR, CHN, and mass facilities. The authors are thankful to the Head, Department of Biotechnology, Kakatiya University, for providing biological activity.

SUPPLEMENTARY INFORMATION

Supplementary material associated with this article can be found, in the online version, at.

CONFLICT OF INTEREST

The authors declare that they have no known competing financial interests or personal relationships that could have appeared to influence the work reported in this paper.

REFERENCES AND NOTES

1. P.C. Sharma, D. Sharma, A. Sharma, M. Bhagat, M. Ola, V.K. Thakur, J.K. Bhardwaj, and R.K. Goyal. Recent advances in microbial toxin-related strategies to combat cancer. *In Seminars in cancer biology. Academic Press*. **2022**, 86, 753-768.
2. R. Palabindela, R.Guda, G. Ramesh, R. Bodapati, S.K. Nukala, P. Myadaraveni, G. Ravi, M. Kasula. Curcumin based pyrazole-thiazole hybrids as antiproliferative agents: Synthesis, pharmacokinetic, photophysical properties, and docking studies. *J. Mol. Struct.* **2023**, 1275, 134633.
3. H.A. Allam, E.E. Aly, A.K. Farouk, A.M. El Kerdawy, E. Rashwan, S.E. Abbass. Design and Synthesis of some new 2, 4, 6-trisubstituted quinazoline EGFR inhibitors as targeted anticancer agents. *Bioorg. Chem*. **2020**, 98, 103726.
4. J. Wang, L. Huang, X. Chen, Y. Yuan, J. Sun, M. Yang. Design, Synthesis and Antitumor Activities of Novel Quinazolinone Derivatives as Potential EGFR Inhibitors. *Chemical Pharmaceut. Bullet*. **2022**, 70, 637-641.
5. R. Palabindela, R. Guda, G. Ramesh, P. Myadaraveni, D. Banothu, G. Ravi, R. Korra, H. Mekala, M. Kasula. Novel tryptanthrin hybrids

bearing aminothiazoles as potential EGFR inhibitors: Design, synthesis, biological screening, molecular docking studies, and ADME/T predictions. *J. Heterocyclic. Chem*. **2022**, 59, 1533-1550.
6. R.T. Dungo, G.M. Keating. *Afatinib: First Global Approval. Drugs* **2013**, 73, 1503-1515.
7. F. Tan, Y. Shi, Y. Wang, L. Ding, X. Yuan, Y. Sun. Icotinib, a selective EGF receptor tyrosine kinase inhibitor, for the treatment of non-small-cell lung cancer. *Future Oncol*. **2015**, 11, 385-397.
8. H. Zhang, W. Gan, D. Fan, P. Zheng, Q. Lv, Q. Pan, W. Zhu. Novel quinazoline-based dual EGFR/c-Met inhibitors overcoming drug resistance for the treatment of NSCLC: Design, synthesis and anti-tumor activity. *Bioorg. Chem*. **2024**, 142, 106938.
9. S.J. Ha, J. Lee, J. Park, Y.H. Kim, N.H. Lee, Y.E. Kim, K.M. Song, P.S. Chang, C.H. Jeong, S.K. Jung. Syringic acid prevents skin carcinogenesis via regulation of NoX and EGFR signaling. *Biochemic.pharmacol*. **2018**, 154, 435-445.
10. E.L.H. Leung, X.X. Fan, M. P. Wong, Z.H. Jiang, Z.Q. Liu, X.J. Yao, L.L. Lu, Y.L. Zhou, L.F. Yau, V. P.C. Tin, L. Liu. Targeting tyrosine kinase inhibitor-resistant non-small cell lung cancer by inducing epidermal growth factor receptor degradation via methionine 790 oxidation. Antioxidants & *Redox Signaling*. **2016**, 24, 263-279.
11. S. Johnpasha, R. Palabindela, M. Azam, R. Kapavarapu, V. Nasipireddy, S.I. Al-Resayes, S. Narsimha. Synthesis and anti-breast cancer evaluation of fused imidazole-imidazo [1, 2-c][1, 2, 3] triazoles: PEG-400 mediated one-pot reaction under ultrasonic irradiation. *J. Mol. Struct*. **2024**, 138440.
12. S. Schacher-Kaufmann, M. Pless. Acute fatal liver toxicity under erlotinib. *Case Rep. Oncol*. **2010**, 3, 182-188.
13. H. Modjtahedi, D.K. Moscatello, G. Box, M. Green, C. Shotton, D.J. Lamb, L.J. Reynolds, A.J. Wong, C. Dean, H. Thomas, S. Eccles. Targeting of cells expressing wild-type EGFR and type- III mutant EGFR (EGFRvIII) by anti-EGFR MAb ICR62: a two- pronged attack for tumour therapy. *Internat. J. Cancer*. **2003**, 105, 273-288.
14. A. Misra, J. Dwivedi, S. Shukla, D. Kishore, S. Sharma. Bacterial cell leakage potential of newly synthesized quinazoline derivatives of 1, 5-benzodiazepines analogue. *J. Heterocyclic Chem*. **2020**, 57, 1545-1558.
15. M.M. Zeydi, N. Montazeri, M. Fouladi. Synthesis and evaluation of novel [1, 2, 4] triazolo [1, 5-c] quinazoline derivatives as antibacterial agents. *J. Heterocyclic Chem*. **2017**, 54, 3549-3553.
16. M. Mohammadi, K.A. Dilmaghani, Y. Sarveahrabi. Synthesis, Antibacterial, and Antifungal Evaluation of Some New Quinazolinone-Azole Hybrids. *Polycycl. Aromat. Comp*. **2024**, 44, 1805-1815.
17. G.B. Gundlewad, B.R. Patil. Synthesis and Evaluation of Some Novel 2-Amino- 4- Aryl Thiazoles for Antitubercular Activity. *J. Heterocyclic Chem*. **2018**, 55, 769-774.
18. I. Dobrescu, E. Hammam, J.M. Dziekan, A. Claës, L. Halby, P. Preiser, Z. Bozdech, P.B. Arimondo, A. Scherf, F. Nardella. Plasmodium falciparum Eukaryotic Translation Initiation Factor 3 is Stabilized by Quinazoline-Quinoline Bisubstrate Inhibitors. *ACS Infectious Diseases*. **2023**, 9, 1257-1266.
19. A.E. Kassab, E.M. Gedawy, H.B. El-Nassan. Synthesis of 4-Heteroaryl–Quinazoline Derivatives as Potential Anti-breast Cancer Agents. *J. Heterocyclic Chem*. **2017**, 54, 624-633.
20. T. Krishnaraj, S. Muthusubramanian. Synthesis of 6-Aryl- 4H-imidazo [1, 2-b][1, 2, 4] triazoles and 6- Aryl- thiazolo [3, 2- b][1, 2, 4] triazoles. *J. Heterocyclic Chem*. **2015**, 52, 1314-1320.
21. M.L. Fascio, M.I. Erre, N.B. D'Accorso. Imidazothiazole and related heterocyclic systems. Synthesis, chemical and biological properties. *Eur. J. Med. Chem*. **2015**, 90, 666-683.
22. I.M. Othman, Z.M. Alamshany, N.Y. Tashkandi, M.A. Gad-Elkareem, S.S. Abd El-Karim, E.S. Nossier. Synthesis and biological evaluation of new derivatives of thieno-thiazole and dihydrothiazolo-thiazole scaffolds integrated with a pyrazoline nucleus as anticancer and multi-targeting kinase inhibitors. *RSC adv*. **2022**, 12, 561-577.
23. L. Xiaofang, L. Bin, L. Haochong, Y. Xianyong, Y. Pinggui. Synthesis of Novel Spiro Thiazolotriazole Derivatives via 1, 3-Dipolar Cycloaddition of Azomethine Ylide. *J. Heterocyclic Chem*. **2012**, 49, 1050-1053.
24. H.A.H. El–Sherif, A.M. Mahmoud, A.A.O. Sarhan, Z.A. Hozien, O.M.A. Habib. One pot synthesis of novel thiazolo [3, 2-b][1, 2, 4] triazoles: A useful synthetic application of the acidified acetic acid method. *J. Sulfur Chem*. **2006**, 27, 65-85.
25. P. Kumar, A. Kumar, J.K. Makrandi. Synthesis and Evaluation of Bioactivity of Thiazolo [3, 2-b]- [1, 2, 4]- triazoles and Isomeric Thiazolo [2, 3-c]- [1, 2, 4] -triazoles. *J. Heterocyclic Chem*. **2013**, 50, 1223-1229.
26. B.S. Chhikara. Synthesis of hybrid Usnic Acid 1, 2, 3-triazole conjugate with cholesterol using Click Chemistry method. *J. Mol. Chem.* **2021**, 1 (1), 101.
27. S. Chirra, R. Gondru, M. Manne, M. Azam, S.I. Al-Resayes, R. Manchal, S. Narsimha. Synthesis of [1, 2, 4] triazolo [3, 4-b][1, 3, 4] thiadiazine-1, 2, 3-triazoles as potent EGFR targeting anti-breast cancer agents. *J. Mol. Struct*. **2024**, 137803.
28. S. Demirayak, G. Zitouni, P. Chevallet, K. Erol, F.S. Kiliç. Synthesis and vasodilatory activity of some thiazolo-triazole derivative. *Farmaco*. **1993**, 48, 707-712.
29. H.A. El-Sherief, B.G. Youssif, S.N.A. Bukhari, A.H. Abdelazeem, M. Abdel-Aziz, H.M. Abdel-Rahman. Synthesis, anticancer activity and molecular modeling studies of 1, 2, 4-triazole derivatives as EGFR inhibitors. *Eur. J. Med. Chem*. **2018**, 156, 774789.
30. M.R. Aouad, H.M. Al-Mohammadi, F.F. Al-Blewi, S. Ihmaid, H.M. Elbadawy, S.S. Althagfan, N. Rezki. Introducing of acyclonucleoside analogues tethered 1, 2, 4-triazole as anticancer agents with dual epidermal growth factor receptor kinase and microtubule inhibitors. *Bioorg. Chem*. **2020**, 94, 103446.
31. B. Banerji, S.K. Killi, A. Katarkar, S. Chatterjee, Y. Tangella, C. Prodhan, K. Chaudhuri. Neo-tanshinlactone D-ring modified novel analogues induce apoptosis in human breast cancer cell via DNA damage. *Bioorg. Med. Chem*. **2017**, 25, 202-212.
32. R.I. Alsantali. Design, Synthesis, and Anticancer Activity of New Quinazoline Derivatives Containing Acetylhydrazide Moiety as EGFR Inhibitors and Apoptosis Inducers. *Russ. J. Bioorg. Chem*. **2023**, 49(3), 645-654.
33. M.S. Karthikeyan. Synthesis, analgesic, anti-inflammatory and antimicrobial studies of 2, 4-dichloro-5-fluorophenyl containing thiazolotriazoles. *Eur. J. Med. Chem*. **2009**, 44, 827-833.
34. E. Ramya Sucharitha, S. Kumar Nukala, N. Swamy Thirukovela, R. Palabindela, R. Sreerama, S. Narsimha. Synthesis and Biological Evaluation of Benzo [d] thiazolyl-Sulfonyl- Benzo [4, 5] isothiazolo [2, 3-c][1, 2, 3] triazole Derivatives as EG FR Targeting Anticancer Agents. *Chemistry Select*. **2023**, 8, 202204256.
35. S. Amudala, R. Palabindela, S. Bhoomandla, N. Kotilingaiah, J. Sandhya, J. Mandala. Synthesis of Novel 2-((3-(Benzofuran-2-yl)-1-phenyl-1 H-pyrazol-4-yl) methylene) hydrazinyl-4-phenylthiazole: Potent EGFR Targeting Anticancer Agents. *Russ. J. Bioorg. Chem*. **2024**, 50, 34-44.
36. S. Johnpasha, R. Palabindela, M. Azam, R. Kapavarapu, V. Nasipireddy, S.I. Al-Resayes, S. Narsimha. Synthesis and anti-breast cancer evaluation of fused imidazole-imidazo [1, 2-c][1, 2, 3] triazoles: PEG-400 mediated one-pot reaction under ultrasonic irradiation. *J. Mol. Struct*. **2024**, 1312, 138440.
37. S.R. Bandi, N. Kavitha, S.K. Nukala, N.S. Thirukovela, R. Manchal, R. Palabindela, S. Narsimha. Synthesis and biological evaluation of novel [1, 2, 3] triazolo-pyrrolo [1, 2-a] pyrido [4, 3-d] pyrimidines as EGFR targeting anticancer agents. *J. Mol. Struct*. **2023**, 1274,134378.
38. V. Rustagi, S.R.R. Gupta, A. Singh, I.K. Singh. Beyond trial and error: Leveraging advanced software for Therapeutic discovery. *Chem. Biol. Lett.* **2025**, 12 (1), 1251.